

Published in final edited form as:

*Nano Lett.* 2011 March 9; 11(3): 1383–1388. doi:10.1021/nl200116d.

## Preparation of Mineralized Nanofibers: Collagen Fibrils Containing Calcium Phosphate

Michael Maas<sup>1,†</sup>, Peng Guo<sup>2,3,†</sup>, Michael Keeney<sup>4</sup>, Fan Yang<sup>4,5</sup>, Tammy M. Hsu<sup>2</sup>, Gerald G. Fuller<sup>1</sup>, Charles R. Martin<sup>3</sup>, and Richard N. Zare<sup>2,‡</sup>

<sup>1</sup> Department of Chemical Engineering, Stanford University, Stanford, CA 94305-5025 USA

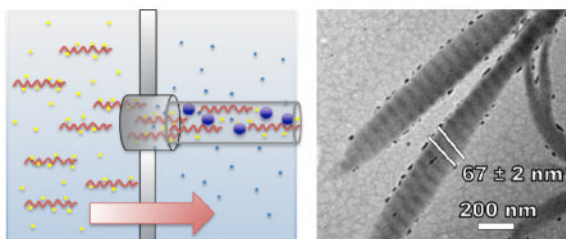
<sup>2</sup> Department of Chemistry, Stanford University, Stanford, CA 94305-5080 USA

<sup>3</sup> Department of Chemistry, University of Florida, Gainesville, FL 32611-7200 USA

<sup>4</sup> Department of Orthopaedic Surgery, Stanford University, Stanford, CA 94305 USA

<sup>5</sup> Department of Bioengineering, Stanford University, Stanford, CA 94305 USA

### Abstract



We report a straightforward, bottom-up, scalable process for preparing mineralized nanofibers. Our procedure is based on flowing feed solution, containing both inorganic cations and polymeric molecules, through a nanoporous membrane into a receiver solution with anions, which leads to the formation of mineralized nanofibers at the exit of the pores. With this strategy, we were able to achieve size control of the nanofiber diameters. We illustrate this approach by producing collagen fibrils with calcium phosphate incorporated inside the fibrils. This structure, which resembles the basic constituent of bones, assembles itself without the addition of noncollagenous proteins or their polymeric substitutes. Rheological experiments demonstrated that the stiffness of gels derived from these fibrils is enhanced by mineralization. Growth experiments of human adipose derived stem cells on these gels showed the compatibility of the fibrils in a tissue-regeneration context.

### Keywords

Biom mineralization; Collagen; Calcium Phosphate; Nanoporous Membrane

<sup>‡</sup>To whom correspondence should be addressed. zare@stanford.edu.

<sup>†</sup>These authors contributed equally to this work and are co-first authors.

Supporting Information Available: Figure S1: SEM images of collagen fibrils prepared using a nanoporous membrane (pore size 200 nm), collagen film prepared without nanoporous membrane and clean PCTE membrane with 200 nm pores. Figure S2: EDS of the collagen fibrils: collagen; collagen/CaP (1 mM CaCl<sub>2</sub> in feed solution); collagen/CaP (5 mM CaCl<sub>2</sub> in feed solution). This material is available free of charge via the Internet at <http://pubs.acs.org>.

Nanofibers can be generated in numerous ways, such as electrospinning and self-assembly and with different materials like natural and artificial polymers, or amphiphilic peptides.<sup>1–6</sup> Mineralization of nanofibers has been pursued with a major goal being the preparation of a material that resembles the basic structure of mammalian bone.<sup>4,7–12</sup> In this paper, we present a new and straightforward method for the preparation of mineralized collagen fibrils that closely resemble natural bone material. Our strategy was based on a nanoporous polycarbonate track-etched (PCTE) membrane that separated two liquids, a feed solution and a receiver solution. This approach was used previously to prepare nanoparticles<sup>13</sup> but we extend it here to produce fibrils. Fibrils were formed by pumping the feed solution through the membrane into the receiver solution. The feed solution contained calcium cations ( $\text{Ca}^{2+}$ ) and monomolecular tropo-collagen. The receiver solution contained phosphate anions ( $\text{HPO}_4^{2-}$ ), which induced precipitation of the inorganic salt along and within the collagen fibrils. This method has the appeal that it is readily scalable.

Organisms produce a wide variety of organic-inorganic hybrid materials called biominerals. The most common biominerals are the phosphate and carbonate salts of calcium that are found in conjunction with organic polymers, such as collagen and chitin, to give structural support to bones and shells. Biomineralization has inspired chemists to seek new synthetic strategies for creating inorganic materials in complex forms, for example by pattern recognition of self-organized organic assemblies.<sup>14,15</sup> Along with the advancement of our understanding of biological processes, the main goal of these studies is to find new materials for bone grafting, tissue engineering, or other medical applications.<sup>16,17</sup>

The nature of the interaction between organic matrix and inorganic mineral in biomineralization processes has long been a subject of debate.<sup>18,19</sup> Early evidence led to the view that crystal growth was guided by epitaxy with the organic matrix as a template.<sup>19–23</sup> Later, several nonclassical crystallization pathways have been proposed for biomineralization.<sup>24–27</sup> In the last several years, evidence for the importance of an amorphous precursor phase has rapidly accumulated and now is the dominant view in the field.<sup>28–31</sup> It has been found that acidic non-collagenous proteins play an important role in facilitating the amorphous phase.<sup>32</sup> Acidic hydrophilic polymers have been used to mimic these noncollagenous proteins. As has been established by several studies,<sup>18,33,34</sup> the role of the acidic polymer is twofold: It suppresses bulk crystallization of the mineral and stabilizes the amorphous phase. With this approach, pre-assembled collagen fibrils could be mineralized with calcium phosphate. This could be achieved with the use of polyanionic polymers like poly-aspartate or poly-lactate.<sup>7–9</sup> As will be seen in what follows, our method removes the need of using polyanionic polymers in preparing fibrils.

Triple-helical single tropo-collagen molecules spontaneously self-assemble into fibrils under the right conditions.<sup>35,10,36–40</sup> In collagen fibrils, each triple helix is shifted relative to its molecular neighbor by 40 nm in the direction of the helix and overlaps the adjacent molecule by 27 nm, which results in the characteristic 67 nm-spaced band pattern of collagen fibrils (Figure 1, scheme). Laterally, the helices are arranged in a hexagonal pattern with respect to each other within the fibril. Collagen fibrils are most stable at moderately basic pH (9–11) and high ion (especially phosphate) concentrations.<sup>41,42</sup>

Using the method presented in this paper, it was possible to incorporate calcium phosphate (CaP), into collagen fibrils without any additional polymers or proteins. We achieved the simultaneous formation of collagen fibrils and amorphous CaP at the exit of the pores in the PCTE membrane. Therefore, we found a new bottom-up approach for the artificial formation of the basic building blocks of bone. We use the abbreviation CaP to denote calcium phosphate, although it is not presently known the exact chemical composition and morphology of this phosphate salt of calcium.

The rheology of gels derived from highly-concentrated fibril suspensions was investigated to understand the mechanical properties of the fibrils. To demonstrate the biomedical usefulness of the fibrils generated with this approach in a tissue-engineering context, human adipose derived stem cells (hADSCs) were grown on substrates made of collagen fibril aggregates.

## Materials

All chemicals were purchased from Sigma Aldrich (St. Louis, MO) and used without further purification. Calcium chloride ( $\text{CaCl}_2$ ) and dibasic sodium monohydrogen phosphate ( $\text{Na}_2\text{HPO}_4$ ) were prepared fresh daily using Millipore water. Type I tropo-collagen from rat tails was purchased from BD Biosciences (Bredford, MA). Stock solutions were 3 mg/mL tropo-collagen in 0.1 M acetic acid. 10x PBS buffer was obtained from Invitrogen (Carlsbad, CA).

## U-tube setup

The U-tube setup consisted of two half U-tubes and a nanoporous membrane sandwiched between the two halves (Figure 1). Polycarbonate track-etched (PCTE) nanoporous membranes (Whatman, Nuclepore Track-Etch Membrane, Florham Park, NJ) with pore diameters between 50 nm and 1  $\mu\text{m}$  are used in our experiments. For the preparation of collagen fibrils, one half of the U-tube was filled with 6-mL feed solution containing 1 mg/mL collagen, 1–20 mM  $\text{CaCl}_2$  and 1 mM HCl (pH 3.0); the other half was filled with 4-mL receiver solution containing 0.66 mM  $\text{Na}_2\text{HPO}_4$  and 1 mM NaOH. A gauge pressure of 250 mbar was created by connecting a compressed air outlet with a pressure reduction valve to the feed solution side of the U-tube. In this way, the feed solution was pumped into the receiver solution according to the applied pressure. Fibrils were collected by filtration through PCTE membranes and dried at room temperature. The PCTE membranes that were used for filtration (not to be confused with the ones used for fibril formation) also served as the substrate for scanning electron microscopy (SEM). To investigate the influence of filtration on artifact formation, different kinds of membranes with different pore sizes were used for the last filtration step in control experiments. Regardless of the type of filter used, the fibrils always had the same appearance.

## SEM

Scanning electron microscopy images were acquired using an FEI XL30 Sirion SEM. Dry samples on carbon sticky tape were sputter-coated for 120 s at 15 mA with Pd/Au. The diameters of the fibrils were evaluated with the software ImageJ.

## TEM

Transmission electron microscopy (TEM) was carried out using a FEI Tecnai G2 F20 X-TWIN. Samples were deposited on formvar carbon-coated copper grids without prior filtration. Coupled to the TEM was selected area electron diffraction (SAED) and energy disperse x-ray spectroscopy (EDS).

## Preparation of gels for rheology

To prepare gels from the fibril suspensions (obtained as described above, using a pore size of 200 nm), the suspensions were dialyzed for 24 h using a seamless cellulose membrane (width = 32 mm; diameter = 20.4 mm; pore size = 4 nm; Fisher Science Education, Rochester, NY). Poly(ethyleneglycol) was the drying agent. The samples were afterwards filtrated through a 50-nm PCTE membrane until they were completely dried. The samples

derived from collagen fibrils were swelled for 1 h in 10x PBS buffer directly before the measurements.

## Rheological measurements

The rheological experiments were carried out using a TA AR-G2 equipped with an 8-mm parallel plate geometry. While the plate geometry was oscillated at a frequency  $\omega$ , we measured the torque (stress) that was required to arrive at a certain deformation (strain). The frequency sweep tests were carried out with a strain of  $\gamma = 0.1$  %.

## Preparation of substrates for stem cell experiments

The fibril scaffolds used for stem-cell culture were prepared by filtering fibril suspensions (obtained as described above, using a pore size of 200 nm) on a 50-nm PCTE nanoporous membrane until the filter surface was completely covered (confirmed by SEM). Three types of fibril samples were prepared into scaffolds: collagen, collagen/CaP (1 mM CaCl<sub>2</sub>), collagen/CaP (5 mM CaCl<sub>2</sub>). Resulting scaffolds were rinsed with deionized water for three times and dried at room temperature.

## Stem Cell Experiments

Human adipose derived stem cells (hADSCs) were isolated from donors and expanded in culture. Cells were cultured in Dulbecco Modified Eagle Medium (DMEM) supplemented with 10% fetal bovine serum, 1% penicillin/streptomycin, and 0.05% fibroblast growth factor. Two-dimensional sheets of fibrils prepared on PCTE filter membranes were placed at the base of a 96 well plate (n=3). Trypsin was added to the hADSCs to remove them from cell culture flasks and  $8 \times 10^3$  cells were seeded per well in 200  $\mu$ l of media further supplemented with  $\beta$ -glycerolphosphate, ascorbic-2-phosphate, dexamethasone, and sodium pyruvate. Cells were cultured for 16 days and media was refreshed every second day.

## Cell Titer

CellTiter 96® (Promega Corp.) assay was performed to quantify cell proliferation at days 5, 11 and 16. Cell media was removed and CellTiter 96® Aqueous One Solution was added to the cells. Quantification was performed with a microplate reader according to the manufacturer's protocol.

## Cell Imaging

Following cell culture, cells were fixed with 4% paraformaldehyde for 15 minutes and washed extensively with phosphate buffered saline solution (PBS). Fluorescein isothiocyanate (FITC) phalloidin (Santa Cruz Biotechnology) was used to stain the actin filaments and samples were mounted with VECTASHIELD® HardSet Mounting Media containing 4',6-diamidino-2-phenylindole (DAPI).

## Statistics

Statistics was performed using MiniTab. A Tukeys comparison determined differences between timepoints and groups ( $p < 0.05$  was considered as statistically different). Data were presented as mean  $\pm$  one standard deviation.

## Results and Discussion

Using the U-tube setup (Figure 1), a feed solution containing 1 mg/mL tropo-collagen in an acidic medium (diluted HCl) was pumped through a nanoporous PCTE membrane into a

receiver solution containing sodium hydroxide at pH 11. Using these parameters, discrete collagen fibrils with a uniform diameter were obtained (Figures 2A and 2B). The diameter of the fibrils could be controlled by choosing the pore diameter of the PCTE membranes while maintaining all other parameters. Collagen fibrils formed using pore diameters of 1  $\mu\text{m}$ , 400 nm, and 200 nm exhibited diameters of  $760 \pm 240$  nm,  $270 \pm 120$  nm and  $120 \pm 30$  nm, respectively. Collagen fibril formation blocked pores smaller than 200 nm. Uncontrolled fibril formation, as was shown by adding 1-mL feed solution to 3-mL receiver solution without membrane, resulted in the precipitation of unstructured collagen aggregates that remained as a dense film on the substrate (Figure S1). The length of the fibril is variable but often exceeds tens of microns.

To obtain mineralized collagen fibrils, calcium chloride ( $\text{CaCl}_2$ ) was added to the feed solution and sodium monohydrogen phosphate ( $\text{Na}_2\text{HPO}_4$ ) was added to the receiver solution. A 200-nm PCTE membrane was used throughout these experiments. The formation of mineralized fibrils was particularly sensitive to the calcium concentration. With lower calcium concentrations (1 mM  $\text{CaCl}_2$  in the feed solution), only the interior of the fibrils was mineralized, as clearly seen by the visible enhancement of the band pattern of the collagen fibrils (compare Figure 2B to Figure 2D, without staining, the band pattern is not visible in unmineralized fibrils with TEM). With higher calcium concentrations (2.5 mM and 5 mM  $\text{CaCl}_2$ ), the fibrils exhibited a mineralized overgrowth (Figures 2E, 2F, 2G, and 2H). A closer examination of the overgrowth revealed segments with spacing on the order of 67 nm, which equals the distance found in the band pattern of collagen fibrils. With  $\text{CaCl}_2$  concentrations as high as 20 mM, plate-like hydroxyapatite crystals precipitated in large bundles that were interconnected by collagen (data not shown).

The existence of calcium phosphate in the fibrils was determined by energy dispersive x-ray spectroscopy (EDS) that was coupled to the TEM. Calcium phosphate was observed in the collagen/CaP (1 mM  $\text{CaCl}_2$ ) and collagen/CaP (5 mM  $\text{CaCl}_2$ ) samples. EDS also revealed that the amounts of calcium phosphate within the fibrils increased with the  $\text{CaCl}_2$  concentration in the feed solution. The EDS of a pure collagen fibrils served as a control sample, in which the characteristic peaks of calcium and phosphate were not observed (Figure S2). Selected area electron diffraction (SAED) showed that the mineral phase was always amorphous (see insets in Figure 2).

The prevalence of the amorphous phase was a result of the rapid flow of the feed solution which created a highly supersaturated phase at the exit of the pores. Heterogeneous nucleation of amorphous calcium phosphate was guided by the gaps between the collagen molecules. The gaps also provided room for growth in an otherwise spatially constrained environment. A rough estimation of the flow rate of the feed solution through a PCTE membrane with a pore size of 200 nm gave a pore velocity of approximately 100  $\mu\text{m/s}$ . This yielded a characteristic extensional flow gradient into such a pore of 1000/s. This rate can be compared to the rotational diffusivity of collagen, which is approximately 810/s<sup>43</sup>. These two rates can be combined to provide an estimate of the Deborah number,  $De = 1.2$ . This dimensionless group, which gauges the propensity of a flow to orient the chains, was somewhat greater than unity, suggesting that the collagen adopted a preferential orientation parallel to the pore axis. In contrast, reaction times of at least four days for the formation of a crystalline phase of calcium phosphate were found in the literature<sup>7</sup>. This fast and coincident formation of fibrils and CaP produced a collagen/CaP composite material without the addition of acidic polymers or natural noncollagenous proteins that are typically involved in bone growth.

To compare the viscoelastic properties of gels produced from the different kinds of fibrils, the shear rheology of gels prepared from highly concentrated fibril suspensions was

investigated. With rheological experiments, it is possible to obtain the dynamic elastic modulus,  $G'$ , and the dynamical viscous modulus,  $G''$ . The rheological experiments revealed that the dynamic moduli strongly increase with increasing calcium phosphate concentration (Figure 3). Compared to pure collagen fibrils, the collagen/CaP fibrils are at least an order of magnitude stiffer. It is known that the stiffness of a gel influences cell differentiation.<sup>44</sup>

The fibrils were tested for their ability to support cell growth in-vitro using human adipose derived stem cells (hADSCs) as a model cell line for tissue engineering. This cell type is found in abundance within the human body and is capable of differentiating down the mesenchymal lineage, making it an excellent candidate for future tissue engineering applications.<sup>45</sup>

Cell growth was quantified using a colorimetric test (CellTiter 96®, Promega, Corp.), which permits a count to be made of viable cells. This assay demonstrated increasing proliferation in all groups at all time points with the exception of collagen fibrils at day 16 (Figure 4B). A trend was also found indicating that the inclusion of calcium phosphate enhanced cell proliferation. Interestingly, only the calcium phosphate containing groups exhibited a statistical increase in alkaline phosphatase activity (Figure 4C), which is an early indicator of bone cell differentiation. Xie et al.<sup>46</sup> have shown that calcium phosphate can induce osteoblast differentiation while Sere et al.<sup>47</sup> have shown that by combining calcium phosphate with collagen, cells upregulate matrix production. Our data also show that increased  $\text{CaCl}_2$  concentration also increased proliferation and alkaline phosphatase production.

Actin staining indicated intimate contact of the cells with the underlying surface, and we also observed out-stretched cells with connecting filopodia. Cells rapidly covered the nanofibrous surface and began to grow in multilayers (Figure 4A).

## Conclusions

We present a new method for preparing mineralized fibrils. This method is able to control the fibril diameter through the choice of the size of the nanopores in a membrane that separates the feed solution from the receiver solution. This work represents to our knowledge the first time that calcium phosphate has been incorporated into collagen fibrils in a one-step process without the use of organic solvents or polyionic additives. This constrained self-assembly process causes the appearance of bands of calcium phosphate inside the fibrils and resembles closely the same structure found in bone. Moreover, this method is simple and can be readily scaled to produce large quantities of nanofibers. In experiments with human adipose derived stem cells we were able to demonstrate the usefulness of fibers generated with our approach in a tissue-engineering context. One possible application might be bone grafting in which we replace missing bone with the mineralized fibrils, which serve as a scaffold for the regeneration of bone structure. We are encouraged to believe that this scalable process for making mineralized fibrils through nanoporous membranes holds much promise for future studies in tissue engineering and in the production of new types of composite materials.

## Supplementary Material

Refer to Web version on PubMed Central for supplementary material.

## Acknowledgments

M. Maas is grateful for financial support from the Deutsche Forschungsgemeinschaft (MA 4795/1-1) and R. N. Zare gratefully acknowledges support from the National Institutes of Health (1R21CA125467).



## References

1. Huang Z, Zhang Y, Kotaki M, Ramakrishna S. *Composites Science and Technology* 2003;63:2223–2253.
2. Teo WE, Ramakrishna S. *Nanotechnology* 2006;17:R89–R106. [PubMed: 19661572]
3. Zhang S, Greenfield MA, Mata A, Palmer LC, Bitton R, Mantei JR, Aparicio C, de La Cruz MO, Stupp SI. *Nature Materials*. 2010
4. Hartgerink JD, Beniash E, Stupp SI. *Science* 2001;294:1684. [PubMed: 11721046]
5. Zhang S. *Nat Biotech* 2003;21:1171–1178.
6. Kim B, Park H, Lee S, Sigmund WM. *Materials Letters* 2005;59:829–832.
7. Olszta MJ, Cheng X, Jee SS, Kumar R, Kim Y, Kaufman MJ, Douglas EP, Gower LB. *Materials Science and Engineering: R: Reports* 2007;58:77–116.
8. Ehrlich H, Hanke T, Born R, Fischer C, Frolov A, Langrock T, Hoffmann R, Schwarzenbolz U, Henle T, Simon P, et al. *Journal of Membrane Science* 2009;326:254–259.
9. Deshpande AS, Beniash E. *Crystal Growth & Design* 2008;8:3084–3090. [PubMed: 19662103]
10. Zhang W, Liao SS, Cui FZ. *Chemistry of Materials* 2003;15:3221–3226.
11. Li X, Xie J, Lipner J, Yuan X, Thomopoulos S, Xia Y. *Nano Letters* 2009;9:2763–2768. [PubMed: 19537737]
12. Fujihara K, Kotaki M, Ramakrishna S. *Biomaterials* 2005;26:4139–4147. [PubMed: 15664641]
13. Guo P, Martin CR, Zhao Y, Ge J, Zare RN. *Nano Letters* 2010;10:2202–2206. [PubMed: 20441186]
14. Mann S, Ozin GA. *Nature* 1996;382:313–318.
15. Estroff LA, Hamilton AD. *Chemistry of Materials* 2001;13:3227–3235.
16. Ripamonti U, van den Heever B, Heliotis M, DAL M, et al. *South African Journal of science* 2002;98:429–433.
17. Ripamonti U, Hari Reddi A. *Critical Reviews in Oral Biology & Medicine* 1997;8:154. [PubMed: 9167090]
18. DiMasi E, Olszta MJ, Patel VM, Gower LB. *CrystEngComm* 2003;5:346–350.
19. Heywood BR, Mann S. *Adv Mater* 1994;6:9–20.
20. Sommerdijk NAJM, With GD. *Chemical Reviews* 2008;108:4499–4550. [PubMed: 18937514]
21. Zhang L, Liu H, Feng X, Zhang R, Zhang L, Mu Y, Hao J, Qian D, Lou Y. *Langmuir* 2004;20:2243–2249. [PubMed: 15835677]
22. Mann S, Archibald DD, Didymus JM, Douglas T, Heywood BR, Meldrum FC, Reeves NJ. *Science* 1993;261:1286. [PubMed: 17731856]
23. Mann S. *Nature* 1993;365:499–505.
24. Cölfen H. *Current Opinion in Colloid & Interface Science* 2003;8:23–31.
25. Tao J, Pan H, Zeng Y, Xu X, Tang R. *The Journal of Physical Chemistry B* 2007;111:13410–13418. [PubMed: 17979266]
26. Cölfen H. *Biomaterialization II* 2007:S. 1–77.
27. Fricke M, Volkmer D. *Biomaterialization I* 2007:S. 1–41.
28. Olszta, Matthew J.; Odom, Damian J.; Douglas, Elliot P.; Gower, Laurie B. *Connective Tissue Research* 2003;44:326–334. [PubMed: 12952217]
29. Gower LB. *Chemical Reviews* 2008;108:4551–4627. [PubMed: 19006398]
30. Weiner S, Mahamid J, Politi Y, Ma Y, Addadi L. *Frontiers of Materials Science in China* 2009;3:104–108.
31. Cheng X, Gower LB. *Biotechnology Progress* 2006;22:141–149. [PubMed: 16454504]
32. Marsh ME. *Protoplasma* 1994;177:108–122.
33. Kato T, Suzuki T, Amamiya T, Irie T, Komiyama M, Yui H. *Supramolecular Science* 1998;5:411–415.
34. Kato K, Eika Y, Ikada Y. *Journal of Materials Science* 1997;32:5533–5543.
35. Bradt J, Mertig M, Teresiak A, Pompe W. *Chemistry of Materials* 1999;11:2694–2701.

36. Gobeaux F, Mosser G, Anglo A, Panine P, Davidson P, Giraud-Guille M, Belamie E. *Journal of Molecular Biology* 2008;376:1509–1522. [PubMed: 18234220]
37. Orgel JPRO, Irving TC, Miller A, Wess TJ. *Proceedings of the National Academy of Sciences* 2006;103:9001–9005.
38. Eglin D, Mosser G, Giraud-Guille M, Livage J, Coradin T. *Soft Matter* 2005;1:129.
39. Kadler KE, Holmes DF, Trotter JA, Chapman JA. *Biochem J* 1996;316:1–11. [PubMed: 8645190]
40. Weis, K.; Pompe, W.; Bradt, J. Process for the preparation of mineralized collagen fibrils and their use as bone substitute material. Google Patents. 2002.
41. Bruns RR, Gross J. *Biopolymers* 1974;13:931–941. [PubMed: 4136772]
42. Chapman JA. *Connective Tissue Research* 1974;2:137–150. [PubMed: 4138005]
43. Fletcher GC. *Biopolymers* 1976;15:2201–2217. [PubMed: 990403]
44. Engler AJ, Sen S, Sweeney HL, Discher DE. *Cell* 2006;126:677–689. [PubMed: 16923388]
45. Strem BM, Hicok KC, Zhu M, Wulur I, Alfonso Z, Schreiber RE, Fraser JK, Hedrick MH. *The Keio journal of medicine* 2005;54:132–141. [PubMed: 16237275]
46. Xie J, Baumann MJ, McCabe LR. *J Biomed Mater Res* 2004;71A:108–117.
47. Serre C, Papillard M, Chavassieux P, Boivin G. *Biomaterials* 1993;14:97–106. [PubMed: 8382091]



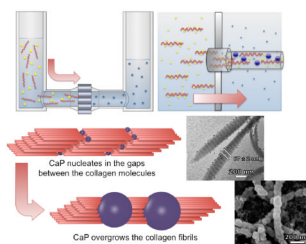


**Figure 1.**

Experimental setup and proposed model for the formation of mineralized collagen fibrils. Amorphous calcium phosphate formed inside or near the exit of the nanopores simultaneously with the self-assembly of collagen fibrils. The fibrils were extruded from the pores in the direction of the feed solution flow. The upper inset is a transmission electron micrograph of the mineralized collagen fibrils showing visual enhancement of the periodic banding structure as a result of the incorporation of CaP. The lower inset is a scanning electron micrograph of the collagen fibrils showing the overgrowth of CaP.

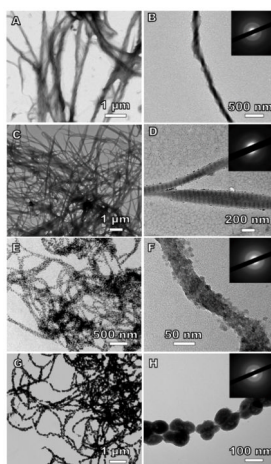


**Figure 2.** Collagen fibrils: (A, B) unmineralized; (C, D) mineralized (1 mM CaCl<sub>2</sub> in feed solution); (E, F) mineralized (2.5 mM CaCl<sub>2</sub>); and (G, H) mineralized (5 mM CaCl<sub>2</sub>). The fibrils were produced using a pore diameter of 200 nm. The insets in (B), (D), (F) and (H) are selected area electron diffraction images showing that the mineral portion is amorphous.

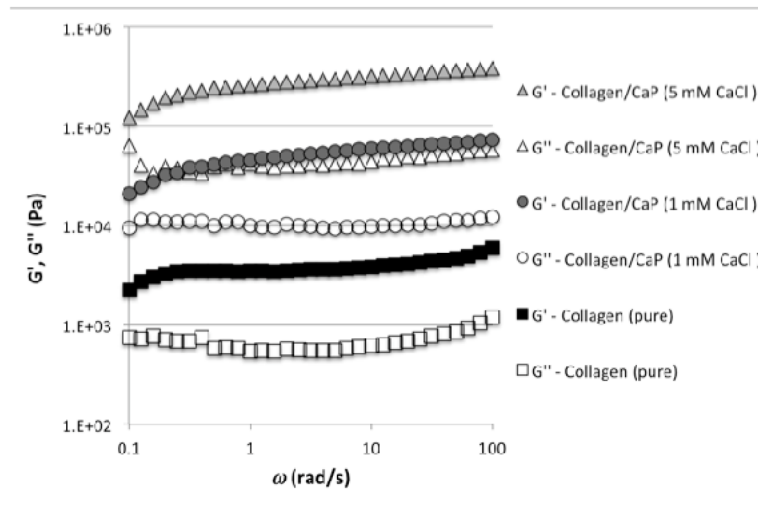


**Figure 3.** Rheological measurements of gels derived from different types of collagen fibrils.

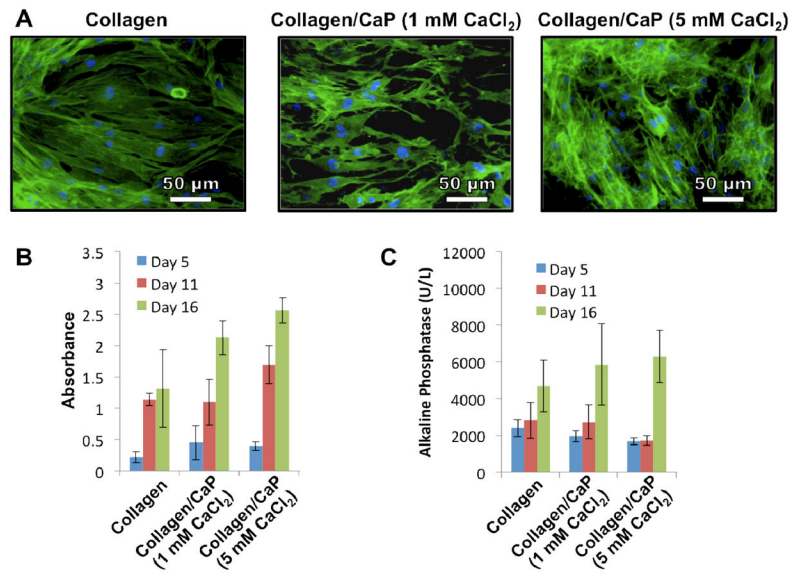


**Figure 4.**

(A) Fluorescent microscopy images of hADSCs cultured on different fibrils in which green indicates actin filaments and blue indicates cell nuclei; (B) Results as a function of time of the CellTiter 96® assay indicating proliferation of hADSCs on collagen fibrils; (C) Alkaline phosphatase production from hADSCs cultured on collagen fibrils as a function of time. The CaCl<sub>2</sub> concentrations refer to the concentrations in the feed solution.